ELSEVIER

International Journal of Heat and Fluid Flow 22 (2001) 201–210

International Journal of HEAT AND FLUID FLOW

www.elsevier.com/locate/ijhff

Cooling effectiveness of a water drop impinging on a hot surface

M. Pasandideh-Fard, S.D. Aziz, S. Chandra *, J. Mostaghimi

Department of Mechanical and Industrial Engineering, University of Toronto, 5 King's College Road, Toronto, Ont., Canada M5S 3G8

Received 7 March 2000; accepted 3 November 2000

Abstract

We studied, using both experiments and a numerical model, the impact of water droplets on a hot stainless steel surface. Initial substrate temperatures were varied from 50°C to 120°C (low enough to prevent boiling in the drop) and impact velocities from 0.5 to 4 m/s. Fluid mechanics and heat transfer during droplet impact were modelled using a "Volume-of-Fluid" (VOF) code. Numerical calculations of droplet shape and substrate temperature during impact agreed well with experimental results. Both simulations and experiments show that increasing impact velocity enhances heat flux from the substrate by only a small amount. The principal effect of raising droplet velocity is that it makes the droplet spread more during impact, increasing the wetted area across which heat transfer takes place. We also developed a simple model of heat transfer into the droplet by one-dimensional conduction across a thin boundary layer which gives estimates of droplet cooling effectiveness that agree well with results from the numerical model. The analytical model predicts that for fixed Reynolds number (*Re*) cooling effectiveness increases with Weber number (*We*). However, for large Weber numbers, when $We \gg Re^{0.5}$, cooling effectiveness is independent of droplet velocity or size and depends only on the Prandtl number.

Keywords: Droplet impact; Spray cooling

1. Introduction

A liquid droplet projected onto a solid surface undergoes rapid deformation as it spreads into a thin film. If the substrate is hotter than the drop, the liquid will cool it. Predicting the degree of cooling requires knowledge both of the area wetted by the droplet and the heat flux from the hot surface to the liquid. Analysis of this problem is both fascinating and complex, coupling free-surface flow, motion of a liquid-solid-vapour contact line, and heat transfer in the liquid drop and solid substrate.

Widespread use of spray cooling in industrial applications such as cooling of turbine blades, fire suppression by sprinkler systems, and quenching of metal castings has motivated many experimental and analytical studies of droplets and sprays impinging on a hot surface. Bolle and Moreau (1982) have reviewed much of the early literature on spray cooling of hot surfaces. Mudawar and Valentine (1989) developed an extensive set of empirical correlations to predict heat transfer rates during quenching with water sprays. Yao and Choi (1987) studied the effect of varying spray droplet diameter and impact velocity by generating mono-dispersed sprays in which all droplets had uniform diameters and velocities. Halvorson et al. (1994) measured heat flux from a hot surface on which a stream of water droplets was impacting. Chandra and Avedisian (1991) photographed impact of droplets on a heated plate. Though most spray cooling studies have been principally concerned with droplets that boil after landing on a hot surface, single-phase heat transfer is often the most important mode of heat transfer. This is usually the case when the objective of spraying an object is to keep it cool and prevent overheating, so that its temperature remains below the boiling point of the liquid.

Several numerical models of droplet impact on a surface, which include heat transfer between the solid and liquid, have been developed. Zhao et al. (1996) formulated a finite-element model of droplets deposited on solid surfaces. Their study was part of an effort to develop a novel technique for depositing solder on circuit boards, and they focused on molten metal droplets impacting on cold surfaces. A number of other investigators, interested primarily in spray forming or coating applications, have also modelled impact, spreading and solidification of molten metal droplets (Trapaga et al., 1992; Liu et al., 1993; Waldvogel and Poulikakos, 1997). Pasandideh-Fard et al. (1998) simulated impact of molten tin droplets on a steel plate, and compared model predictions with photographs of impacting droplets. Bussmann et al. (1999) developed a three-dimensional fluid flow code that they used to simulate water droplet impact on an inclined substrate and a step.

Little use has been made of numerical models of droplet impact in studying cooling of hot surfaces by impinging water droplets. DiMarzo et al. (1993) developed a model of cooling under a droplet evaporating while resting on a hot surface. However, in many applications, droplets do not remain on the

* Corresponding author. Tel.: +1 416 978 5742; fax: +1 416 978 7753.
E-mail address: chandra@mie.utoronto.ca (S. Chandra).

0142-727X/01/$ - see front matter
PII: S0142-727X(00)00086-2

Notation

A	wetted area of substrate
A_{max}	maximum wetted area of substrate
c_p	specific heat of droplet
D	diameter of spreading droplet, measured at droplet-substrate interface
D_0	diameter of spherical droplet
D_{max}	maximum droplet diameter after spreading on the surface
k	thermal conductivity of drop
m	mass of droplet
p	pressure
q''	heat flux from surface to droplet
r	radial co-ordinate
t	time
t^*	dimensionless time ($=tV_0/D_0$)
t_c	droplet spread time
$T_{d,i}$	initial droplet temperature
T_w	surface temperature
$T_{w,i}$	initial surface temperature
V_o	droplet impact velocity

Greeks

δ_T	thermal boundary layer thickness
δ_u	velocity boundary layer thickness
ΔT	$T_{w,i} - T_{d,i}$
ε	cooling effectiveness
γ	surface tension
μ	viscosity of drop
ρ	density of drop
θ_a	advancing liquid–solid contact angle
ξ	spread factor ($= D/D_o$)
ξ_{max}	maximum spread factor

Dimensionless numbers

Pr	Prandtl Number ($=\mu c_p/k$)
Re	Reynolds Number ($=\rho V_o D_o/\mu$)
We	Weber Number ($=\rho V_o^2 D_o/\gamma$)

surface after impact but rebound (for example, when the surface is facing downwards or moving). All heat transfer takes place during the brief period when the droplet touches the surface and is due to convection and conduction within the drop rather than evaporation. Evaporation is a relatively slow process, limited by the rate of vapour diffusion away from the droplet surface, and the mass of liquid vaporised during the few milliseconds it takes for a droplet to spread on a hot surface and rebound is negligible.

The principal objective of our study was to simulate, using a numerical model, impact of water droplets on a hot steel plate and to validate results from the model by comparing them with experimental observations. We photographed 2.0 mm diameter water drops as they landed on a stainless steel plate, and measured surface temperature variations. Initial substrate temperatures were varied between 50°C and 120°C; localised cooling under impacting drops reduced the plate temperature sufficiently to prevent the onset of boiling at even the highest temperatures in this range. Impact velocities ranged from 0.5 to 4 m/s, low enough to prevent droplets from shattering during impact. Fluid flow and heat transfer during droplet impact were modelled using a "Volume-of-Fluid" (VOF) code, which has been described in detail earlier (Pasandideh-Fard et al., 1996, 1998). We compared model predictions of droplet shape and substrate temperature variation during impact with experimental measurements.

Often, when designing spray-cooling systems, we need to make quick estimates of heat transfer during droplet impact and to predict the effect of changing spray parameters such as droplet diameter, impact velocity and liquid thermophysical properties. A simple analytical model is much more convenient for this purpose than a complex numerical simulation. We developed such a model and confirmed that it gave good estimates of heat transfer from the substrate by comparing its predictions with those from our numerical model. The analytical model allows us to easily scale the results of this study to droplets with other sizes, velocities, and physical properties than those examined in experiments.

2. Numerical method

Fluid flow and heat transfer in an impinging droplet were modelled using a finite difference solution of the momentum and energy equations in an axisymmetric system of co-ordinates. The fluid flow was assumed laminar and incompressible. The flow Reynolds number (assuming radial flow over a flat plate in the droplet after impact) was estimated to be at most 10^4, too small to induce turbulence. Heat transfer in the droplet was modelled by solving the energy equation; viscous dissipation compared to the conduction and convection heat transfers was neglected. Heat transfer within the substrate was by conduction only. Details of the fluid flow and heat transfer model have been given earlier (Pasandideh-Fard et al., 1996, 1998).

The surface profile of the deforming droplet was defined using the "fractional volume of fluid" scheme (Nichols et al., 1980). In this method, a scalar function F is defined whose value is equal to the fractional volume of the cell occupied by the fluid. F is assumed to be unity when a cell is fully occupied by the fluid and zero for an empty cell. Cells with values of $0 < F < 1$ contain a free surface. An equivalent surface pressure, calculated from the Laplace equation, replaced normal stresses at a free surface; tangential stresses were neglected. Experimentally measured values of the dynamic liquid–solid contact angle, θ, were prescribed as a boundary condition. Liquid density and surface tension were assumed constant. Liquid viscosity, however, was assumed to vary with temperature. The energy equation in the droplet was modelled by using the enthalpy method, described in Pasandideh-Fard et al. (1998). In this method the original energy equation is converted to an equation with only one dependent variable: the enthalpy. The free surface of the droplet was assumed to be adiabatic. The thermal properties of the droplet and substrate were assumed to vary with temperature. Thermal contact resistance between the droplet and substrate was assumed to be zero. Properties of droplet and substrate materials (water and stainless steel) were taken from Batchelor (1967) and Incropera and DeWitt (1996), respectively.

The momentum and energy equations were solved on an Eulerian rectangular, staggered mesh in an axisymmetric coordinate system using the modified SOLA–VOF method. Details of the computational steps required for advancing the solution through one time step have been given earlier (Pasandideh-Fard et al., 1998). The droplet was discretised using a variable mesh with a grid spacing that varies gradually from 0.01 mm close to the substrate to 0.05 mm within the droplet. The mesh size was determined on the basis of a mesh refinement study in which the grid spacing was progressively decreased until further reductions made no significant change in

the predicted droplet shape during spreading. A detailed description of such a mesh refinement study has been given earlier by Bussmann et al. (1999). The substrate mesh had the same resolution, and was extended far enough that its boundaries could be assumed to be at constant temperature. Numerical computations were performed on a Sun ULTRA ENTERPRISE 450 workstation. Typical CPU times ranged from 1 to 2 h.

3. Experimental method

Water droplets, 2.0 mm in diameter, were formed at the tip of a 33 gauge stainless steel hypodermic needle and allowed to detach and fall under their own weight onto a stainless steel test surface. Droplets could be released from a height of up to 1 m, to obtain impact velocities ranging from 0.5 to 4.0 m/s. The droplets fell inside a 25 mm diameter aluminium tube which prevented air currents from changing their trajectory, ensuring that they landed at the same location on the substrate. We measured droplet impact velocity by taking multiple exposures of a falling droplet prior to its impact on the surface. By measuring the distance travelled in a known time interval we could determine droplet velocity. These measured velocities agreed closely with those calculated for a droplet falling under the effect of gravity. Droplet impact velocities were reproducible to within ± 0.01 m/s.

Photographs of impacting droplets were taken using a single-shot technique that has been described in detail earlier (Chandra and Avedisian, 1991). As a droplet fell it interrupted a laser beam, sending a signal to a time delay unit. This unit first opened the shutter of a Nikon E2N digital still camera, and then after a pre-set time triggered an 8 μs duration flash to take a single picture of an impacting droplet. By varying the time delay different stages of droplet impact were recorded. The camera recorded high-resolution images (1280×1000 pixels) which were transferred to a computer for analysis. Image analysis software (NIH Image, National Institutes of Health) was used to measure droplet dimensions as they deformed. The resolution of our contact diameter measurements, corresponding to the size of one pixel of the digital image, was within ± 0.1 mm.

The test surface was a 50 mm square stainless steel plate, 6.3 mm thick. The upper surface was polished with 600 grit emery

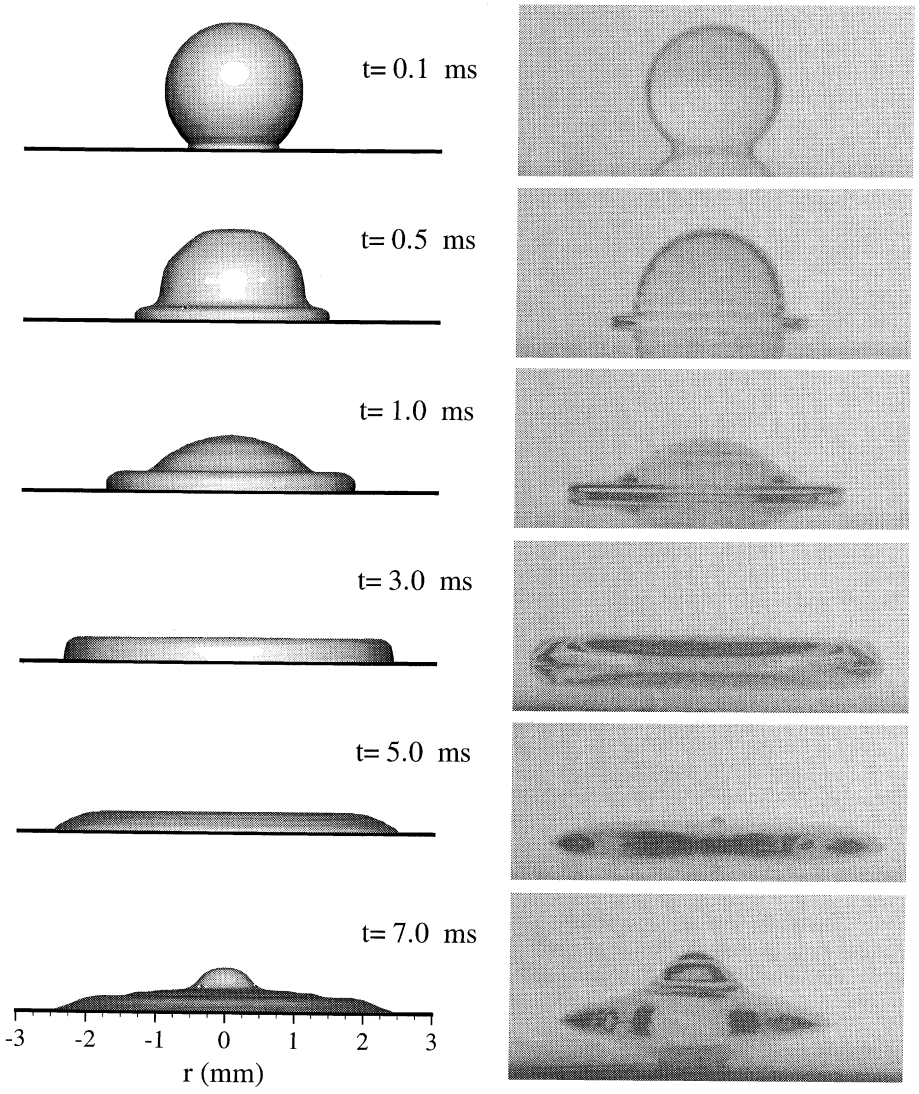

Fig. 1. Computer generated images and photographs of a 2.0 mm diameter water droplet impacting with a velocity of 1.3 m/s on a stainless steel surface initially at a temperature of 120°C.

cloth. The surface was mounted on a copper block, which was heated by cartridge heaters inserted into it, and whose temperature was regulated by an electronic temperature controller. We varied the initial substrate temperature from 50°C to 120°C in this study. Substrate temperature variation during impact was measured using a commercially available ''eroding'' thermocouple (E 12-3-K-7, Nanmac Corp., Framingham, MA) which has a response time of 10 μs (as specified by the manufacturer). The technique was similar to that used earlier by Chen and Hsu (1995) and Qiao and Chandra (1996). The thermocouple consists of two fine wires of chromel and alumel alloys, separated by an insulating mica layer and encased in a stainless steel sheath. The thermocouple was inserted vertically through the steel substrate and its tip ground flat, level with the test surface. The thermocouple wires smeared across the insulation separating them during grinding, forming a bare thermocouple junction flush with the test surface. Water droplets were dropped precisely onto this junction. The thermocouple output during droplet impact was amplified and recorded using a data acquisition system. Temperature measurements were estimated to be accurate to within ±1°C.

4. Results and discussion

Fig. 1 shows images, generated by the numerical model, of successive stages of impact of a 2.0 mm diameter water droplet with initial temperature $T_{d,i} = 25$°C and velocity $V_o = 1.3$ m/s, landing on a stainless steel surface initially at temperature $T_{w,i} = 120$°C. Each image is compared with the photograph of a droplet taken at the same time (t) after the instant of impact. Reflections of droplets can be seen in the polished stainless steel surface in the photographs. A droplet reached its maximum extent at approximately $t = 3.0$ ms, by which time surface tension and viscous forces overcame inertia, so that fluid started to accumulate at the leading edge of the spreading droplet. Surface tension finally caused droplets to draw inwards and begin to lift off the surface ($t = 7.0$ ms). Comparison of computer generated images with photographs showed that the model predicted droplet shape during impact with reasonable accuracy. Quantitative comparisons of measured and calculated droplet spread diameters have also shown good agreement previously (Pasandideh-Fard et al., 1996).

Results from the numerical model were used to gain insight into fluid flow during droplet impact. Calculated velocity distributions and instantaneous streamlines within the droplet are displayed in Fig. 2, at the same times seen in Fig. 1. Corresponding pressure distributions within the droplet are given in Fig. 3. Following initial contact between the droplet and surface downward motion of the fluid was arrested by the solid substrate that diverted the flow radially. Radial velocities increased from zero at the centre to approximately twice the impact velocity at the leading edge of the spreading fluid disk. Fluid was accelerated by a favourable pressure gradient

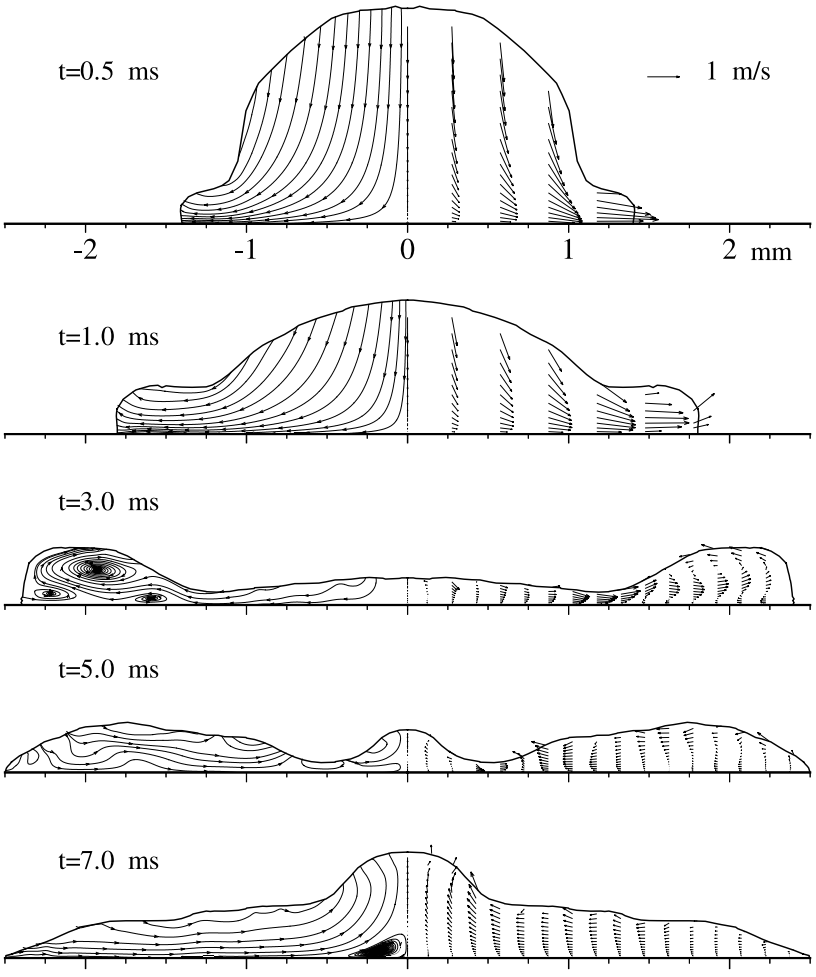

Fig. 2. Calculated velocity vector and instantaneous streamlines in a 2.0 mm diameter water droplet impacting with a velocity of 1.3 m/s on a stainless steel surface initially at a temperature of 120°C.

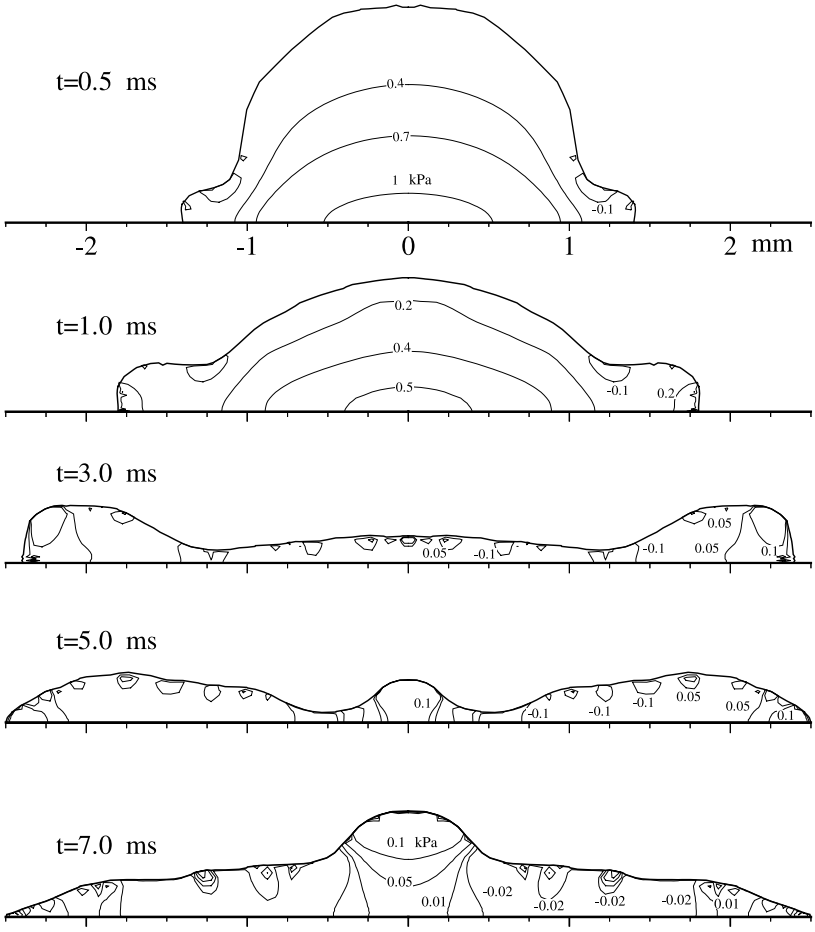

Fig. 3. Calculated pressure distribution in a 2.0 mm diameter water droplet impacting with a velocity of 1.3 m/s on a stainless steel surface initially at a temperature of 120°C.

($\partial p/\partial r < 0$) as seen in Fig. 3 at $t = 0.5$ and 1.0 ms. At later times viscous forces overcame fluid inertia and surface tension dominated further flow. Curvature of the free liquid surface was highest at the leading edge (see Fig. 3 at $t = 1.0$ ms) producing a region of high pressure. This created an adverse pressure gradient ($\partial p/\partial r > 0$), as seen in Fig. 3 at $t = 3.0$ ms, decelerating the fluid. Fluid near the substrate lacked sufficient momentum to overcome this pressure gradient, resulting in boundary layer separation and the formation of several recirculation zones (see Fig. 2, $t = 3.0$ ms). After this time droplet recoil occurred and fluid started to flow back towards the centre ($t = 5.0$ and 7.0 ms).

Calculated droplet shapes and temperature distributions within the droplet and substrate are seen in Fig. 4, at the same times as the previous figures. At early stages of impact ($t = 0.5$ and 1 ms) the bulk of liquid in the drop remained at its initial temperature of 25°C. The isotherm corresponding to 26°C was assumed to represent the edge of a thermal boundary layer in contact with the substrate, and is marked in Fig. 4. The thermal boundary layer thickness (δ_T) was approximately 0.04 mm and remained almost constant during spreading ($t < 3.0$ ms). It was only when the droplet had reached its maximum extent and begun to recoil that fluid recirculation disrupted this regular boundary layer.

Isotherms within the substrate were quite uniform under the droplet and the cooling induced by the droplet penetrated to a depth of approximately 0.6 mm by $t = 7.0$ ms (see Fig. 4). Fig. 5 shows the substrate surface temperature distribution at five instants of time during droplet impact. The surface temperature at the centre of the drop, initially 120°C, dropped rapidly to 103°C within 0.1 ms after impact. The substrate temperature increased radially and reached its initial value of 120°C at the edge of the drop. As the droplet spread further the area cooled by it increased, and the temperature at the centre of the drop decreased further. Calculated heat fluxes from the surface to the drop are plotted in Fig. 6, at the same times shown in Fig. 5. Very high heat fluxes were obtained immediately following droplet impact: at $t = 0.1$ ms they ranged from 8 to 9 MW/m^2. Heat flux was relatively constant under the drop, but increased near its periphery where cold liquid first contacted the hot substrate producing the maximum heat transfer rates. Parts of the substrate not in contact with liquid were assumed adiabatic so that heat flux was zero at all times. Heat flux was reduced rapidly as droplet spread progressed; liquid temperature increased and flow velocity decreased, reducing both conduction and convection. By $t = 3$ ms the droplet reached its maximum spread after which the heat flux remained relatively unchanged.

Predictions of substrate temperature variation were validated by comparing them with measurements made using a thermocouple placed on the substrate at the point of droplet impact. Fig. 7 shows measured temperature variations for a stainless steel surface initially at 120°C during impact of water droplets with velocities ranging from 1.3 to 4 m/s. The temperature dropped very rapidly after impact, reaching a minimum within 0.3 ms, and then remained constant. Impact

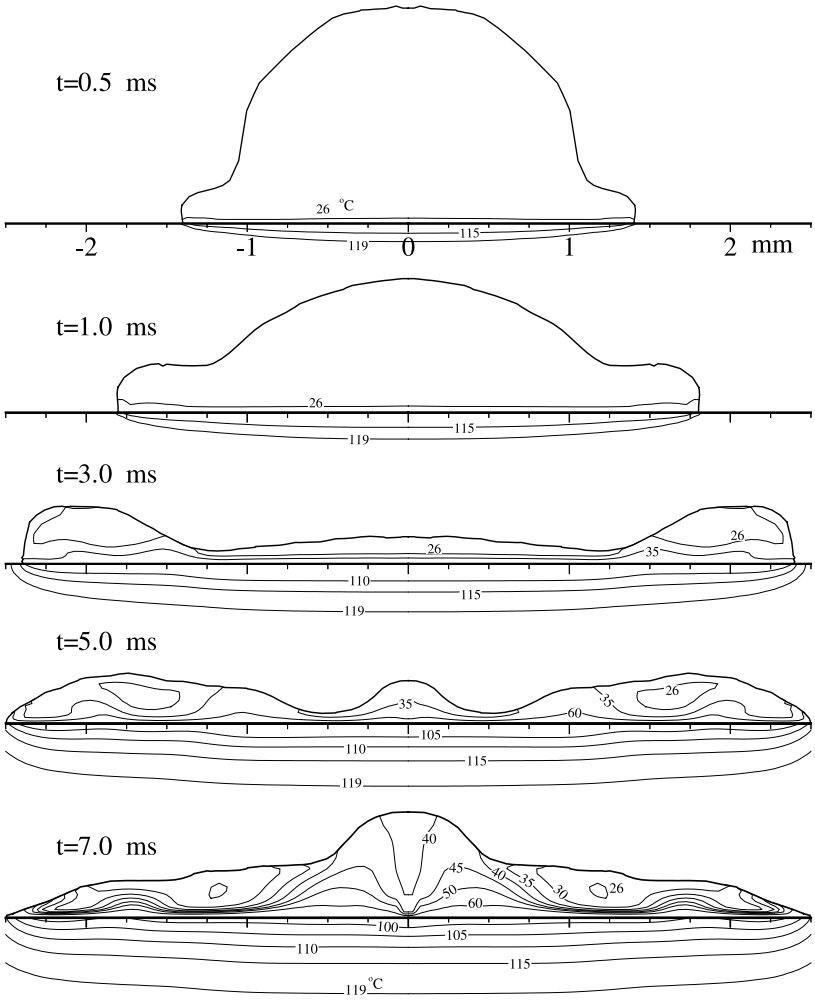

Fig. 4. Calculated temperature distribution in a 2.0 mm diameter water droplet at 25°C impacting with a velocity of 1.3 m/s on a stainless steel surface initially at a temperature of 120°C.

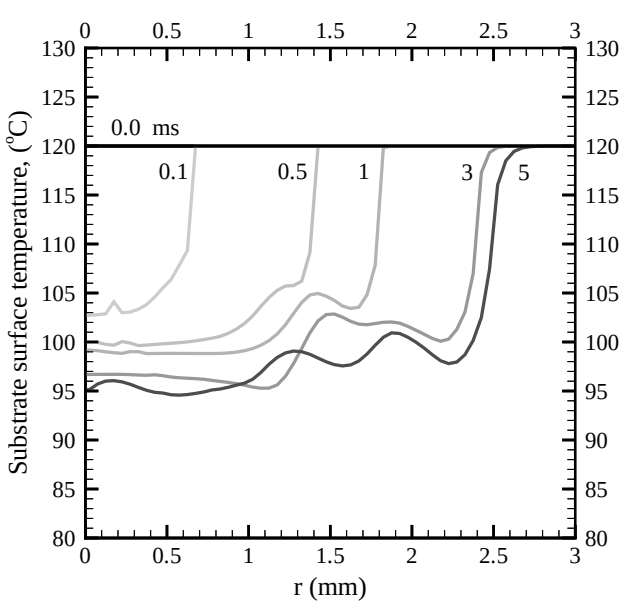

Fig. 5. Substrate surface temperature distribution at five instants following the 1.3 m/s impact of a 2.0 mm diameter water droplet at 25°C on a stainless steel surface initially at a temperature of 120°C.

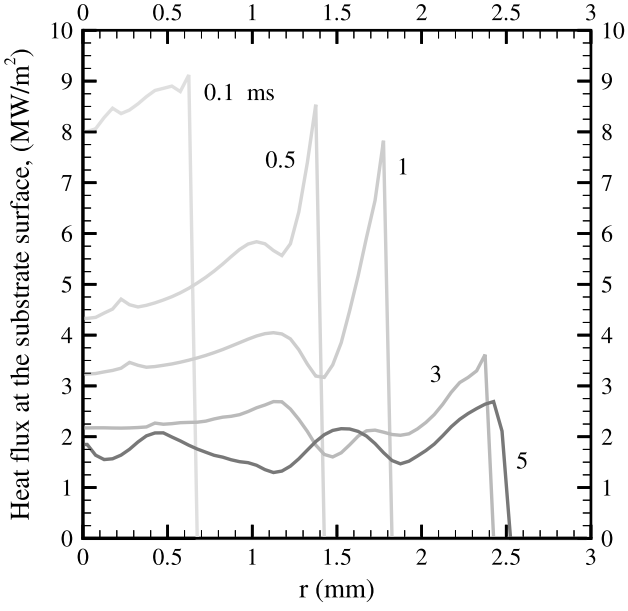

Fig. 6. Substrate heat flux distribution at five instants following the 1.3 m/s impact of a 2.0 mm diameter water droplet at 25°C on a stainless steel surface initially at a temperature of 120°C.

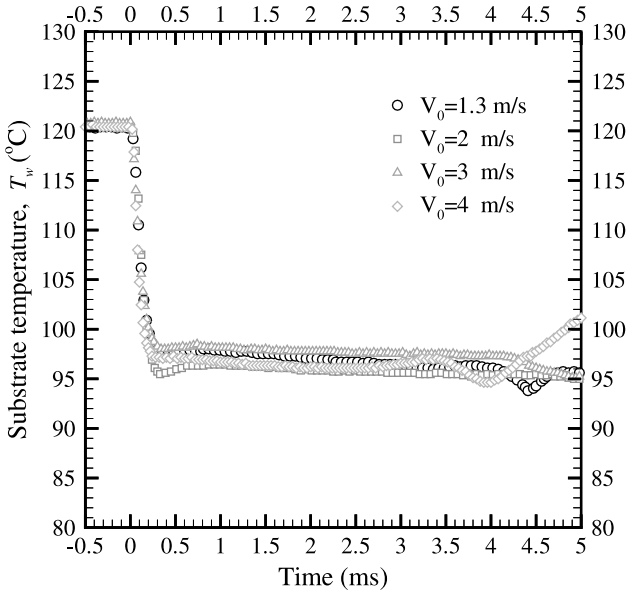

Fig. 7. Measured variation of substrate temperature at the point of impact of 2.0 mm diameter water droplets at 25°C, landing with velocity V_o on a stainless steel surface initially at a temperature of 120°C.

velocities in the range of our experiments had only a small effect on surface cooling. Raising droplet velocity enhanced substrate cooling slightly, though given the uncertainties in initial droplet temperature (±1°C) and substrate temperature measurement (±1°C) it is difficult to clearly distinguish this effect in Fig. 7.

Calculated surface temperatures agreed well with measurements. Fig. 8 is a comparison of measured and calculated surface temperature variations for $V_o = 1.3$ m/s and $T_{w,i} = 120$°C, showing good agreement. There was a small dip in the temperature at $t = 4.5$ ms, produced when droplet impact was complete and recoil started, directing colder liquid onto the centre of the drop. This effect was seen repeatedly in experiments and was reproduced by the model. Similar agreement was observed at all velocities and substrate temperatures used in this study. We used the temperature decrease ($\Delta T_w = T_{w,i} - T_w$), 1 ms after impact, as a measure of surface cooling following droplet impact. Fig. 9 shows measured values of ΔT_w compared with predictions from the model for $V_o = 0.5$–4 m/s and $T_{w,i} = 50°, 80°$ and 120°C. ΔT_w is seen to increase slightly with impact velocity, a trend that was confirmed by the numerical model.

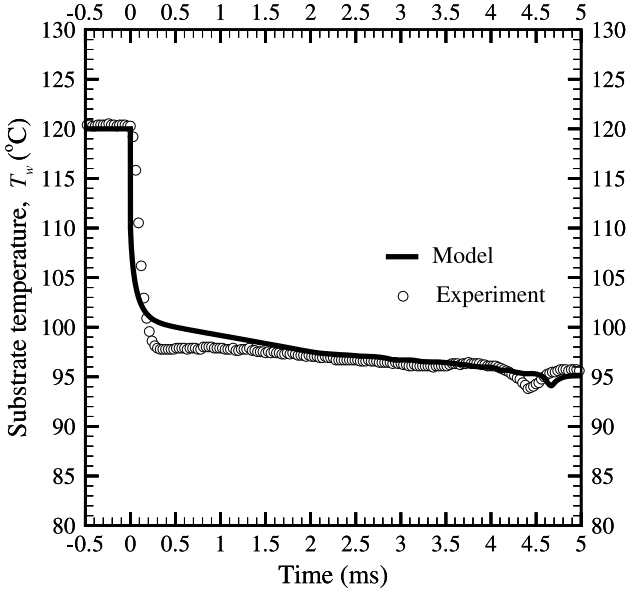

Fig. 8. Comparison between measured and calculated variation of substrate temperature at the point of impact of a 2.0 mm diameter water droplet at 25°C, landing with a velocity of 1.3 m/s on a stainless steel surface initially at a temperature of 120°C.

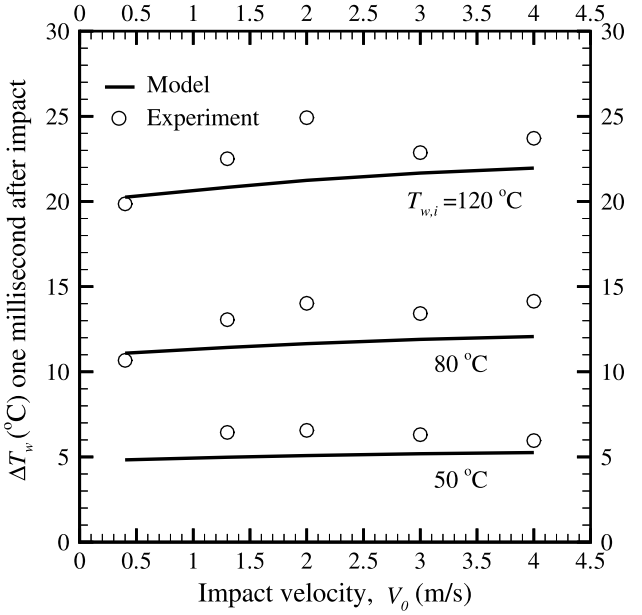

Fig. 9. Comparison between measured and calculated drop in substrate temperature at the point of impact of 2.0 mm diameter water droplets at 25°C, landing with velocity V_o on a stainless steel surface initially at a temperature $T_{w,i}$.

Impact velocity had little effect on heat flux from the surface. However, the area wetted by the droplet grows larger as droplet velocity is raised, thereby increasing heat transfer from the substrate to the droplet. The evolution of droplet diameter during impact is shown in Fig. 10 for four values of V_o: 1.3, 2.0, 3.0 and 4.0 m/s. Droplet spread was quantified by measuring the diameter (D) of the surface area in contact with the drop and normalising it by initial droplet diameter (D_o) to give the "spread factor" $\xi = D/D_o$. The spread factor is shown as a function of the dimensionless time $t^* = tV_o/D_o$ in Fig. 10. During impact the spread factor first increased as the droplet spread on the surface and then decreased as it recoiled. The maximum spread factor (ξ_{max}) increased with impact velocity, from a value of 2.6 for $V_o = 1.3$ m/s to approximately 4.8 at $V_o = 4.0$ m/s. The scatter in the data was highest at $V_o = 4.0$ m/s because the rim of the droplet became wavy and irregular reducing the repeatability of the measurements. The dimensionless time taken for droplets to reach their maximum spread (t_c^*) was estimated by Pasandideh-Fard et al. (1996) to be $t_c^* = 2.67$, based on a simple model of droplet impact. In reality t_c^* increased slightly with impact velocity, and ranged from 2 to 4 in our experiments (see Fig. 10). However, for simplicity in our analysis we assumed that $t_c^* = 2.67$ represents a reasonable order-of-magnitude estimate, independent of impact velocity.

A quantitative measure of how well an impinging droplet cools a surface is the "cooling effectiveness" (ε)

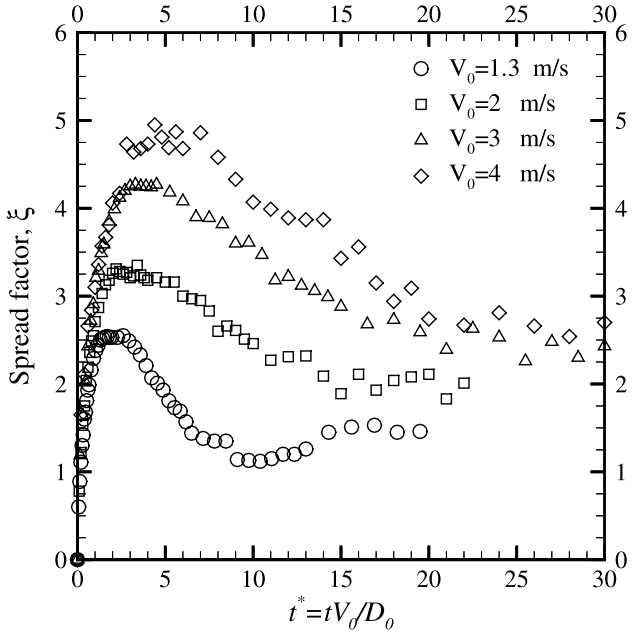

Fig. 10. Evolution of the measured spread factor during the impact of 2.0 mm water droplets landing with velocity V_o on a stainless steel surface initially at 120°C.

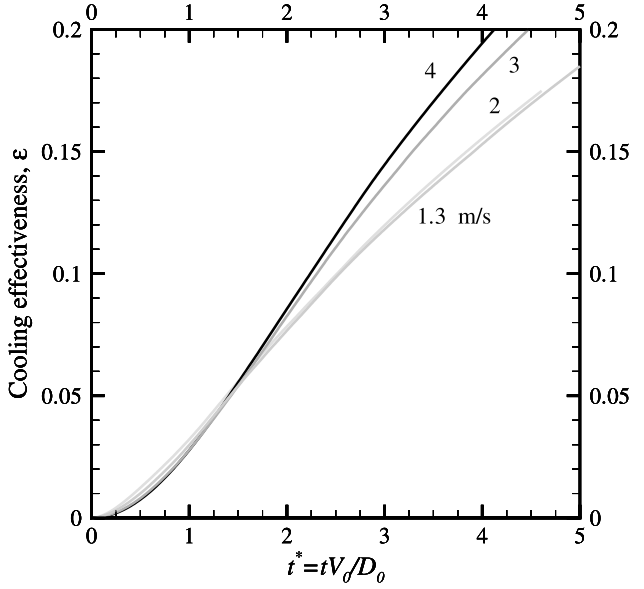

Fig. 11. Evolution of the calculated cooling effectiveness during the impact of 2.0 mm water droplets on a stainless steel surface initially at 120°C.

$$\varepsilon = \frac{\int_0^t \int_0^A q'' \,\mathrm{d}A \,\mathrm{d}t}{mc_p \Delta T}, \tag{1}$$

where q'' is the heat flux from the surface, A the wetted area, m and c_p the droplet mass and specific heat, respectively, and ΔT the difference between the initial droplet and substrate temperatures ($\Delta T = T_{w,i} - T_{d,i}$). The numerator in Eq. (1) gives the actual heat transfer from the substrate to the droplet in time t, which we can either calculate from numerical simulations or estimate from a simple analytical model described below. The denominator represents the maximum heat transfer possible in theory (assuming that there is no phase change). Fig. 11 shows the variation of ε during impact of a 2 mm water droplet on a stainless steel substrate initially at 120°C, calculated from the numerical model for several velocities. Cooling effectiveness increases with impact velocity, because of the larger surface area covered by the drop.

We developed a simple analytical expression to estimate ε in terms of dimensionless numbers that can be used to scale the effect of droplet size, velocity and physical properties on heat transfer during droplet impact. To compare the relative importance of these parameters we considered only the heat transfer that occurs during droplet spreading; fluid flow during this period is driven by inertial forces and not greatly affected by gravity and surface tension (Qiao and Chandra, 1996). After spreading the droplet may come to rest, recoil, or splash. Its behaviour is highly dependent on factors such as surface wettability, roughness and orientation, which are specific to a given application.

The total heat transfer (q_c) from a hot substrate to an impinging droplet during the time it spreads to its maximum extent can be estimated as follows:

$$q_c = \int_0^{t_c} \int_0^{A_{max}} q'' \,\mathrm{d}A \,\mathrm{d}t \approx q'' A_{max} t_c, \tag{2}$$

where A_{max} is the maximum wetted area, equal to $\pi D_{max}^2/4$, and t_c is the time required for the droplet to reach its maximum extent (when $D = D_{max}$). Pasandideh-Fard et al. (1996) assumed $t_c = (8D_o)/(3V_o)$, which corresponds to $t_c^* = 2.67$, a reasonable median value in our experiments (see Fig. 10). Substituting these values in Eq. (2) gives:

$$q_c \approx \frac{2\pi}{3} \frac{D_o D_{max}^2}{V_o} q''. \tag{3}$$

The heat flux is given by:

$$q'' = k \frac{T_{w,i} - T_{d,i}}{\delta_T} = k \frac{\Delta T}{\delta_T}, \tag{4}$$

in which k is the liquid thermal conductivity. The thermal boundary layer thickness (δ_T) can be obtained from a similarity solution for heat transfer during axisymmetric stagnation point flow (White, 1991):

$$\delta_T = \frac{\delta_u}{Pr^{0.4}}, \tag{5}$$

where Pr is the Prandtl number ($Pr = \mu c_p/k$), δ_u the velocity boundary layer thickness, can be estimated from the axisymmetric stagnation point flow solution (Pasandideh-Fard et al., 1996):

$$\delta_u = \frac{2D_o}{Re^{0.5}}. \tag{6}$$

Re is the Reynolds number ($Re = \rho V_o D_o/\mu$). Substituting for δ_u in Eq. (5) gives an analytical expression for the thermal boundary layer thickness during droplet spreading:

$$\delta_T = \frac{2D_o}{Re^{0.5} Pr^{0.4}}. \tag{7}$$

Substituting values of D_o and V_o from our experiments in Eq. (7) gives $\delta_T = 0.035$ mm, in good agreement with predictions from the numerical model where δ_T ranged from 0.035 to 0.04 mm (see Fig. 4 at $t = 0.5$–1.0 ms). Heat flux during droplet spreading can therefore be obtained by substituting Eq. (7) in Eq. (4) giving

$$q'' = k \frac{\Delta T}{2D_o} Re^{0.5} Pr^{0.4}. \tag{8}$$

The maximum possible heat transfer from the substrate to a droplet is

$$mc_p(T_{w,i} - T_{d,i}) = \frac{\pi}{6} D_o^3 \rho c_p \Delta T. \quad (9)$$

Combining Eqs. (3), (8) and (9) we obtain a simple expression for the cooling effectiveness

$$\varepsilon = \frac{2}{Re^{0.5} Pr^{0.6}} \xi_{max}^2. \quad (10)$$

Pasandideh-Fard et al. (1996) derived an analytical expression for ξ_{max}, based on a simple energy conservation model of droplet impact,

$$\xi_{max} = \frac{D_{max}}{D_o} = \sqrt{\frac{We + 12}{3(1 - \cos\theta_a) + 4(We/Re^{0.5})}}, \quad (11)$$

where θ_a is the advancing liquid–solid contact angle during droplet spreading on the surface. Substituting Eq. (11) into Eq. (10) yields

$$\varepsilon = \frac{2}{Pr^{0.6}} \left[\frac{We + 12}{3(1 - \cos\theta_a) Re^{0.5} + 4We} \right]. \quad (12)$$

We measured the advancing contact angle from photographs of impacting droplets for V_o in the range 1.3–4 m/s using the method described in detail by Pasandideh-Fard et al. (1996). During spreading of water droplets on a stainless steel surface the advancing contact angle (θ_a) had a value of $110° \pm 10°$, and was independent of impact velocity. We therefore used a value of $\theta_a = 110°$ in all calculations.

Eq. (12) gave estimates of cooling efficiency that agreed reasonably well with predictions from the numerical model. Comparisons were done for droplet sizes in the range $0.1 < D_o < 2$ mm and impact velocities $1 < V_o < 8$ m/s, representative of typical spray cooling applications. The results are given in Table 1.

Variation of the cooling effectiveness with dimensionless numbers *Re*, *We* and *Pr*, calculated from Eq. (12), is shown in Fig. 12. The shaded region indicates the range of parameters covered by our experiments. The Prandtl number *Pr* is a fluid property and therefore fixed for a given liquid. As seen from the figure, increasing *Re* while holding *We* and *Pr* constant decreased the cooling effectiveness. We can offer a physical explanation for this trend by noting that for a given liquid *We* and *Re* can be varied only by changing impact velocity and droplet diameter. *Re* can be increased while holding *We* constant by decreasing V_o and simultaneously increasing D_o. As a consequence of decreased impact velocity the maximum spread factor (ξ_{max}) is reduced, and therefore the cooling effectiveness. We conclude that small, fast droplets cool more effectively than large, slow droplets, a result that seems to agree with physical intuition. Yao and Choi (1987) measured heat flux from a hot surface to a simulated spray in which all droplets had uniform diameter and velocity. In the range of their experiments (with $We = 100$–200 and $Re = 2000$–3000) they found that heat flux increased with impact velocity for single-phase heat transfer.

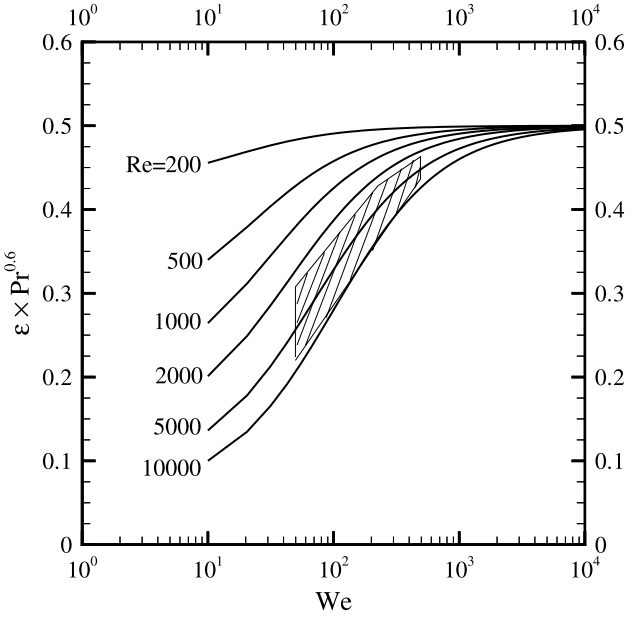

Fig. 12. Cooling effectiveness variation with *Re*, *We*, and *Pr*, calculated from Eq. (12).

At large impact velocities, when $We \gg Re^{0.5}$ and $We \gg 12$, Eq. (12) reduces to

$$\varepsilon = \frac{1}{2Pr^{0.6}}. \quad (13)$$

Cooling effectiveness is then independent of droplet dimensions, and depends only on fluid properties. Note, however, that large values of *We* lead to the onset of droplet splashing. It has been shown (Mundo et al., 1995; Stow and Hadfield, 1981) that droplets shatter during impact when the so-called "splashing parameter", proportional to $WeRe^{0.5}$, exceeds a critical value. The value of $WeRe^{0.5}$ required to produce splashing depends on a number of parameters, including droplet physical properties and substrate roughness. Modelling fluid mechanics and heat transfer during splashing is an extremely complex problem, and a two-dimensional numerical

Table 1
Comparison of the values of cooling effectiveness from the numerical model and analytical expression, Eq. (12)

Case	D_0 (mm)	V_0 (m/s)	*Re*	*We*	ϵ (Eq. (12))	ϵ (numerical model)
1	2.0	1.3	2908	47	0.097	0.106
2	2.0	2.0	4474	111	0.115	0.105
3	2.0	3.0	6711	249	0.131	0.120
4	2.0	4.0	8949	443	0.140	0.125
5	0.5	1.3	727	12	0.102	0.088
6	0.5	2.0	1119	28	0.108	0.098
7	0.5	3.0	1678	62	0.119	0.131
8	0.5	4.0	2237	111	0.129	0.136
9	0.1	2.0	224	5.5	0.142	0.114
10	0.1	4.0	447	22	0.131	0.123
11	0.1	6.0	671	50	0.135	0.161
12	0.1	8.0	895	89	0.141	0.185

model would no longer be adequate to estimate surface cooling under these circumstances.

5. Conclusions

We have developed a numerical model of heat transfer during droplet impact, and confirmed that it can be used to accurately simulate experimental observation of water droplets landing on a hot stainless steel surface. Both simulations and experiments have shown that impact velocity has only a very weak effect on substrate temperature variation and heat flux. The principal effect of raising impact velocity is that it produces greater droplet spread, increasing the wetted area across which heat takes place. We have also developed a simple model of heat transfer into the droplet by one-dimensional conduction across a thin boundary layer which gives estimates of heat transfer that agree well with results from the numerical model. This analytical model predicts that for fixed Re, cooling effectiveness increases with We. However, for large Weber numbers, when $We \gg Re^{0.5}$, cooling effectiveness is independent of droplet velocity or size during impact and depends only on Pr.

Acknowledgements

Financial support of Materials and Manufacturing Ontario (MMO) is gratefully acknowledged.

References

Batchelor, G.K., 1967. An Introduction to Fluid Dynamics. Cambridge University Press, Cambridge.

Bolle, L., Moreau, J.C., 1982. Spray cooling of hot surfaces. Multiphase Science and Technology 1, 1–97.

Bussmann, M., Mostaghimi, J., Chandra, S., 1999. On a three-dimensional volume tracking model of droplet impact. Physics of Fluids 11, 1406–1417.

Chandra, S., Avedisian, C.T., 1991. On the collision of a droplet with a solid surface. Proceedings of the Royal Society of London A 432, 13–41.

Chen, J.C., Hsu, K.K., 1995. Heat transfer during liquid contact on superheated surfaces. ASME Journal of Heat Transfer 117, 693–697.

DiMarzo, M., Tartarini, P., Liao, Y., Evans, D., Baum, H., 1993. Evaporative cooling due to a gently deposited droplet. International Journal of Heat and Mass Transfer 36, 4133–4139.

Halvorson, P.J., Carson, R.J., Jeter, S.M., Abdel-Khalik, S.I., 1994. Critical heat flux limits for a heated surface impacted by a stream of liquid droplets. ASME Journal of Heat Transfer 116, 679–685.

Incropera, F.P., DeWitt, D.P., 1996. Fundamentals of Heat and Mass Transfer, IV ed., Wiley, New York.

Liu, H., Lavernia, E.J., Rangel, R.H., 1993. Numerical simulation of substrate impact and freezing of droplets in plasma spray processes. Journal of Physics D: Applied Physics 26, 1900–1908.

Mundo, C., Sommerfield, M., Tropea, C., 1995. Droplet-wall collisions: experimental studies of the deformation and breakup process. International Journal of Multiphase Flow 21, 151–173.

Mudawar, I., Valentine, W.S., 1989. Determination of the local quench curve for spray cooled metallic surfaces. Journal of Heat Treating 7, 107–121.

Nichols, B.D., Hirt, C.W., Hotchkiss, R.S., 1980. SOLA-VOF: A solution algorithm for transient fluid flow with multiple free boundaries. Los Alamos Scientific Laboratory, LA-8355, UC-32 and UC-34.

Pasandideh-Fard, M., Bhola, R., Chandra, S., Mostaghimi, J., 1998. Deposition of tin droplets on a steel plate: simulations and experiments. International Journal of Heat and Mass Transfer 41, 2929–2945.

Pasandideh-Fard, M., Qiao, Y.M., Chandra, S., Mostaghimi, J., 1996. Capillary effects during droplet impact on a solid surface. Physics of Fluids 8, 650–659.

Qiao, Y.M., Chandra, S., 1996. Boiling of droplets on a hot surface in low gravity. International Journal of Heat and Mass Transfer 39, 1379–1393.

Stow, C.D., Hadfield, M.G., 1981. An experimental investigation of fluid flow resulting from the impact of a water drop with an unyielding dry surface. Proceedings of the Royal Society A 373, 419–441.

Trapaga, G., Matthys, E.F., Valencia, J.J., Szekely, J., 1992. Fluid flow, heat transfer and solidification of molten metal droplets impinging on substrates:comparison of numerical and experimental results. Metallurgical Transactions B 23B, 701–718.

Waldvogel, J.M., Poulikakos, D., 1997. Solidification phenomena in piciliter size solder droplet deposition on a composite substrate. International Journal of Heat and Mass Transfer 40, 295–309.

White, F.M., 1991. Viscous Fluid Flow, second ed. McGraw Hill, New York, 158–160.

Yao, S.C., Choi, K.J., 1987. Heat transfer experiments of monodispersed vertically impacting sprays. International Journal of Multiphase Flow 13, 639–648.

Zhao, Z., Poulikakos, D., Fukai, J., 1996. Heat Transfer and fluid dynamics during the collision of a liquid droplet on a surface – I. Modeling. Modeling International Journal of Heat and Mass Transfer 39, 2771–2789.